(19) LE GOUVERNEMENT DU GRAND-DUCHÉ DE LUXEMBOURG
Ministère de l'Économie

(11) N° de publication : **LU503346**

(12) **BREVET D'INVENTION** **B1**

(21) N° de dépôt: LU503346

(22) Date de dépôt: 13/01/2023

(51) Int. Cl.:
C25B 3/25, G16C 20/10, C25B 1/02

(30) Priorité:

(43) Date de mise à disposition du public: 13/07/2023

(47) Date de délivrance: 13/07/2023

(73) Titulaire(s):
JIANGXI UNIVERSITY OF SCIENCE AND TECHNOLOGY – 341000 Ganjiang City, Jiangxi (Chine)

(72) Inventeur(s):
LIU Chao – Chine, WANG Daoseng – Chine, CHEN Mingwei – Chine, XU Tao – Chine, LIAO Mengqi – Chine

(74) Mandataire(s):
Patent42 SA – 4081 Esch-sur-Alzette (Luxembourg)

(54) **A METHOD FOR CONSTRUCTING AN EFFICIENT ELECTROCATALYST FOR ACID-BASE ALL-ENVIRONMENT OXYGEN REDUCTION REACTION.**

(57) The present invention discloses a method for constructing an acid-base all- environment efficient oxygen reduction reaction electrocatalyst, which belongs to the field of catalyst technology. The invention first constructs a pre-screening model for all ORR catalysts; screens the catalyst models based on ΔEf < 0eV and ΔEb>Ecoh; then screens the catalysts sequentially based on ΔE*O2 < -0.5eV, ΔE*O2 < ΔE*H2O, ΔE*O2 > - 1.5eV (acidic) or ΔE*OH > -3.5eV (basic), ΔG*OH > 0.4eV, ΔG*OH < 1.6eV, ΔG*OOH→H2O2>ΔG2 screening catalysts; finally, the acid-base all-environment efficient oxygen reduction reaction electrocatalysts were screened according to η acid < 0.8V and η base < 0.8V. The present invention is based on computer to carry out catalyst screening research, which has the advantages of low resource consumption, low carbon and environmental protection, high accuracy and high repeatability.

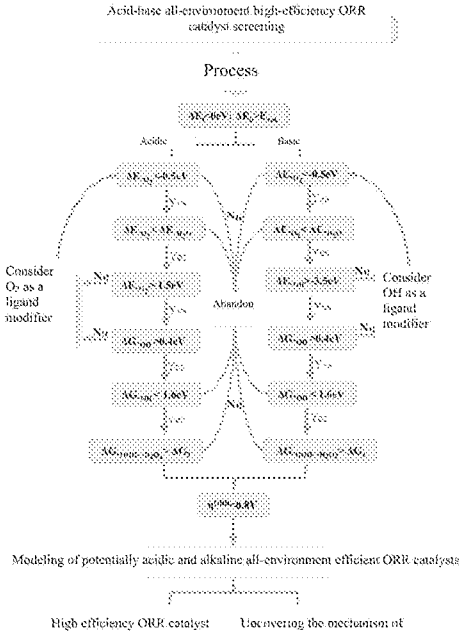

FIG.1

DESCRIPTION

LU503346

A METHOD FOR CONSTRUCTING AN EFFICIENT ELECTROCATALYST FOR ACID-BASE ALL-ENVIRONMENT OXYGEN REDUCTION REACTION

FIELD OF THE INVENTION

The present invention belongs to the field of catalyst technology, and in particular relates to a method of constructing an acid-base all-environment efficient oxygen reduction reaction electrocatalyst.

BACKGROUND OF THE RELATED ART

Fossil fuel combustion produces a large amount of carbon, nitrogen and sulfur containing exhaust gas, on the one hand, the exhaust gas emissions take away a lot of heat energy, resulting in energy waste; on the other hand, toxic exhaust gas, such as CO, NO_X, SO_2 will lead to serious environmental problems, even non-toxic gases, such as CO_2 will cause the greenhouse effect. Moreover, traditional fossil fuels are non-renewable resources, and the increasing depletion of resources will definitely lead to an energy crisis. Therefore, there is an urgent need for human society to develop new energy sources to alleviate the growing energy crisis and environmental problems.

As one of the ideal devices for efficient utilization of clean energy (hydrogen energy), hydrogen-oxygen fuel cells play an important role in meeting the urgent need for sustainable energy because of their high energy conversion efficiency, high power density, and clean environment. However, the slow kinetic cathodic oxygen reduction reaction (ORR) is one of the key factors hindering the widespread application of hydrogen-oxygen fuel cells. The ORR equilibrium potential is 1.23V/0.402V in acidic/alkaline environment respectively, i.e., the reaction kinetics of ORR in alkaline environment is faster than that in acidic environment. However, the acidic environment has a higher power density than the alkaline environment. In addition, the conductivity of OH- in the alkaline environment is lower compared to that of H+ in the acidic environment. Also, H_2 and O_2 must be ultra-pure in the alkaline environment, and the presence of CO_2 in the gas source can lead to carbonate precipitation in the membrane. Thus, it can be seen that both acidic and alkaline solution environments have their own advantages, and Pt-based catalysts are currently the mainstream ORR electrocatalysts

in the market for general use in acidic and alkaline environments. However, Pt is a precious metal and its large-scale commercial application is seriously hindered by its scarce resources, high cost, susceptibility to poisoning by CO in the gas source, low durability, etc.

Therefore, for the constraint bottleneck of hydrogen-oxygen fuel cells, it is necessary to design a rapid screening process of an acid-base all-purpose ORR diatomic catalyst with high catalytic efficiency and high stability based on the abundant resources of transition metal Tm and strong multi-electron activity characteristics, combined with the high atomic dispersion rate, active site utilization and strong synergistic effect of diatomic catalysts

SUMMARY OF THE INVENTION

The existing technology is based on a large number of experimental attempts, which leads to the waste of many resources such as human, material and financial resources due to the existence of certain unknowns, and faces many challenges such as the ambiguity of the catalytic mechanism. In response to the shortcomings of the existing technology, the present invention provides a method for constructing an acid-base all-environment high-efficiency oxygen reduction reaction electrocatalyst, carries out theoretical research based on the first nature principle, provides a screening method for predicting a high-performance acid-base all-environment ORR catalyst model, explores the catalytic mechanism, and provides effective guidance for experimental synthesis.

To achieve the above purpose, the present invention provides the following solutions:

One of the objects of the present invention is to provide a method for constructing an acid-base all-environment efficient oxygen reduction reaction electrocatalyst, the described method being a screening method for N-ligand bimetallic atom co-doped graphene catalysts, comprising the steps of:

(1) Pre-screening models of all ORR catalysts with different bimetallic combinations and different N coordination cases were constructed by VESTA, and the structures were optimized based on the first-nature principle;

(2) Calculation of formation energy ΔE_f and binding energy ΔE_b for the pre-screened models described; screening of stable catalyst models based on $\Delta E_f < 0eV$ and $\Delta E_b > E_{coh}$ (metal cohesion energy);

(3) Construct the adsorption model of catalyst for O_2 in different adsorption modes and optimize the structure (choose the lowest energy adsorption model), calculate the

adsorption energy of catalyst for O_2 ΔE_{*O_2}; screen the catalyst model according to ΔE_{*O_2}<-0.5eV to ensure the effective adsorption and activation of catalyst for O_2;

(4) Construct the H_2O adsorption model and optimize the structure, calculate the H_2O adsorption energy of the catalyst ΔE_{*H_2O}; in order to avoid solvent passivation of the catalyst and ensure the recyclability of the catalyst, select the catalyst model with weak or no H_2O adsorption according to ΔE_{*O_2}< ΔE_{*H_2O};

(5) Classification of the catalyst model into acidic (pH=0) and basic (pH=14) environments:

a. Acidic environment: According to Sabatier's principle, too strong O_2 adsorption will lead to difficult product desorption. Screen the catalyst for proper oxygen adsorption according to ΔE_{*O_2}>-1.5eV, if ΔE_{*O_2}<-1.5eV, consider the possibility of using O_2 as ligand modified catalyst and proceed to step (3) for further screening.

b. Alkaline environment: too strong OH adsorption may passivate the catalyst and make the catalysis difficult to cycle. Construct a model for OH adsorption by the catalyst and optimize the structure, calculate the OH adsorption energy ΔE_{*OH}, screen the catalyst for proper OH adsorption according to ΔE_{*OH}>-3.5eV, if ΔE_{*OH}<-3.5eV means OH is difficult to desorb, re-enter OH as ligand to continue screening in step (3).

(6) Considering the effect of zero-point vibrational energy and entropy on Gibbs free energy, the OH adsorption model is further calculated to calculate the OH adsorption free energy ΔG_{*OH}, and the catalyst with relatively high catalytic activity is screened according to ΔG_{*OH}>0.4eV. If ΔG_{*OH}<0.4eV, η is necessarily greater than 0.8V, the catalyst does not have high activity, Acidic environments can be considered for the possibility of O2 as a ligand, while basic environments can be considered for the possibility of OH as a ligand, proceed to step (3) to continue the screening.

(7) Screen the catalyst according to ΔG_{*OH}<1.6eV, if ΔG_{*OH}>1.6eV, according to the volcano graph of η vs. ΔG_{*OH}, η must be greater than 0.8V, indicating that the catalyst has a weak adsorption capacity for oxygen, small activation O_2 capacity and low catalytic activity, so discard this part of the catalyst.

(8) The generation of side reaction H_2O_2 will corrode the catalyst and affect the durability of the catalyst, so the possibility of generating H_2O_2 should be minimized; calculate the Gibbs free energy $\Delta G_{*OOH\rightarrow H_2O_2}$ for $OOH\rightarrow H_2O_2$ and the reaction energy ΔG_2 for the second electron step of the main reaction, and screen the catalyst with low side reaction rate according to $\Delta G_{*OOH\rightarrow H_2O_2}$>$\Delta G_2$.

(9) Calculate the magnitude of the overpotential η and screen the acid-base all-environment efficient oxygen reduction reaction electrocatalysts according to η_{acid} < 0.8

V and η_{base} < 0.8 V.

Further, the formula for calculating the formation energy ΔE_f described in step (2) is shown in Eq. 01; and the formula for calculating the binding energy ΔE_b described in Eq. 02 to Eq. 03 is shown in.

$$\Delta E_f = E_{Tm_1Tm_2\text{-}N_x\text{-}C_{6\text{-}x}\text{-}gra} + (4+x)\,\mu_C - (E_{gra} + x\mu_N + \mu_{Tm_1} + \mu_{Tm_2}) \quad \text{Eq.01;}$$

$$\Delta E_{b_1} = E_{Tm_2\text{-}N_x\text{-}C_{6\text{-}x}\text{-}gra} + \mu_{Tm_1} - E_{Tm_1Tm_2\text{-}N_x\text{-}C_{6\text{-}x}\text{-}gra} \quad \text{Eq.02;}$$

$$\Delta E_{b_2} = E_{Tm_1\text{-}N_x\text{-}C_{6\text{-}x}\text{-}gra} + \mu_{Tm_2} - E_{Tm_1Tm_2\text{-}N_x\text{-}C_{6\text{-}x}\text{-}gra} \quad \text{Eq.03;}$$

$E_{Tm1Tm2\text{-}Nx\text{-}C6\text{-}x\text{-}gra}$ and E_{gra} refer to the system energy of the N-C coordination environment with double Tm atoms synergistically constructing doped graphene-type diatomic catalysts and defect-free graphene G_{ra}, respectively; μ_C and μ_N refer to the system energy of a single C atom and 1/2 N_2 molecule in graphene Gra, respectively; μ_{Tm_1} and μ_{Tm_2} refer to the energy of single-atom metal Tm_1 and Tm_2; $E_{Tm_2\text{-}N_x\text{-}C_{6\text{-}x}\text{-}gra}$ and $E_{Tm_1\text{-}N_x\text{-}C_{6\text{-}x}\text{-}gra}$ refer to the system energy of N-C coordination double Tm atom co-doped graphene catalyst with Tm_1 and Tm_2 vacancy defects, respectively.

Further, the adsorption energy ΔE_{*O_2} of the catalyst for O_2 as described in step (3) is calculated as shown in Eq. 04.

$$\Delta E_{*O_2} = E_{*O_2\text{-}Tm_1Tm_2\text{-}N_x\text{-}C_{6\text{-}x}\text{-}gra} - E_{Tm_1Tm_2\text{-}N_x\text{-}C_{6\text{-}x}\text{-}gra} - E_{O_2} \quad \text{Eq.04;}$$

$E_{*O_2\text{-}Tm_1Tm_2\text{-}N_x\text{-}C_{6\text{-}x}\text{-}gra}$ is the total system energy of O_2 adsorption by the catalyst, and E_{O_2} is the energy of a single O_2 molecule.

Further, the adsorption energy ΔE_{*H_2O} of H_2O by the catalyst described in step (4) is calculated as shown in Eq. 05.

$$\Delta E_{*H_2O} = E_{*H_2O\text{-}Tm_1Tm_2\text{-}N_x\text{-}C_{6\text{-}x}\text{-}gra} - E_{Tm_1Tm_2\text{-}N_x\text{-}C_{6\text{-}x}\text{-}gra} - E_{H_2O} \quad \text{Eq.05;}$$

$E_{*H_2O\text{-}Tm_1Tm_2\text{-}Nx\text{-}C_{6\text{-}x}\text{-}gra}$ is the total system energy of H_2O adsorption by the catalyst, and E_{H_2O} is the energy of a single H_2O molecule

Further, the OH adsorption energy ΔE_{*OH} described in step (5) is calculated as shown in Eq. 06.

$$\Delta E_{*OH} = E_{*OH\text{-}Tm_1Tm_2\text{-}N_x\text{-}C_{6\text{-}x}\text{-}gra} - E_{Tm_1Tm_2\text{-}N_x\text{-}C_{6\text{-}x}\text{-}gra} - E_{OH} \quad \text{Eq.06;}$$

$E_{*OH\text{-}Tm_1Tm_2\text{-}N_x\text{-}C_{6\text{-}x}\text{-}gr}$a is the total system energy of OH adsorption by the catalyst, and E_{OH} is the energy of a single OH.

Further, the OH adsorption free energy ΔG_{*OH} described in step (6) is calculated as shown in Eq. 07.

$\Delta G_{*OH}=G_{*OH\text{-}Tm_1Tm_2\text{-}N_x\text{-}C_{6\text{-}x}\text{-}gra} - G_{Tm_1Tm_2\text{-}N_x\text{-}C_{6\text{-}x}\text{-}gra}-(G_{H_2O} - 1/2G_{H_2})$ Eq.07;

$G_{*OH\text{-}Tm_1Tm_2\text{-}N_x\text{-}C_{6\text{-}x}\text{-}gra}$ and $G_{Tm_1Tm_2\text{-}N_x\text{-}C_{6\text{-}x}\text{-}gra}$ are the Gibbs free energies of the system with OH adsorbed by the catalyst and the catalyst system alone, respectively, and G_{H_2O} and G_{H_2} are the Gibbs free energies of individual H_2O and H_2 molecules, respectively.

Further, the Gibbs free energy $\Delta G_{*OOH\rightarrow H_2O_2}$ for $OOH\rightarrow H_2O_2$ and the reaction energy ΔG_2 for the second electron step of the main reaction described in step (8) are calculated as shown in Eq. 08 and Eq. 09.

$\Delta G_{*OOH\rightarrow H_2O_2}=G_{H_2O_2}+G_{Tm_1Tm_2\text{-}N_x\text{-}C_{6\text{-}x}\text{-}gra}-(G_{*OOH\text{-}Tm_1Tm_2\text{-}N_x\text{-}C_{6\text{-}x}\text{-}gra}+(0.5G_{H_2}-0.0592\times pH))$ Eq.08;

$\Delta G_2=G_{*O\text{-}Tm_1Tm_2\text{-}N_x\text{-}C_{6\text{-}x}\text{-}gra}+G_{H_2O}-(0.5G_{H_2}-0.0592\times pH)-G_{*OOH\text{-}Tm_1Tm_2\text{-}N_x\text{-}C_{6\text{-}x}\text{-}gra}$ Eq.09

$G_{*OOH\text{-}Tm_1Tm_2\text{-}N_x\text{-}C_{6\text{-}x}\text{-}gra}$ and $G_{*O\text{-}Tm_1Tm_2\text{-}N_x\text{-}C_{6\text{-}x}\text{-}gra}$ refer to the Gibbs free energy of the system in which the catalyst adsorbs OOH and O, respectively, and $G_{H_2O_2}$ refers to the Gibbs free energy of a single H_2O_2 molecule.

Further, the equations for calculating η_{acid} and η_{base} as described in step (9) are shown in Eq. 10 to Eq. 12 as follows.

$\Delta G=\Delta E_{DFT}+\Delta ZPE-T\Delta S+\Delta G_U+\Delta G_{pH}$ Eq.10;

$\eta_{酸}= 1.23\ V + [\Delta G_1, \Delta G_2, \Delta G_3, \Delta G_4]_{max}/e$ Eq.11;

$\eta_{碱}=0.402\ V + [\Delta G_1, \Delta G_2, \Delta G_3, \Delta G_4]_{max}/e$ Eq.12;

ΔE_{DFT} is the reaction energy obtained based on the DFT calculation, ΔZPE and ΔS are the changes of zero-point vibrational energy and entropy before and after the reaction, respectively, T is the temperature, and ΔG_U and ΔG_{pH} are the effects of potential and pH on the reaction free energy ΔG, respectively.

Further, ΔG_U and ΔG_{pH} are calculated as shown in Eq. 13 and Eq. 14.

$\Delta G_U=-neU$ Eq.13;

$\Delta G_{pH}=k_BT\times ln10\times pH$ Eq.14;

n is the number of electron transfer, U refers to the applied potential, and k_B refers to the Boltzmann constant.

Other catalysts can be screened by referring to this method.

Beneficial effects of the present invention.

(1) The present invention is based on a high-performance computer for catalyst screening research, which is different from pure experiments with large resource consumption and "three waste emissions", the invention has the advantage of low

carbon and environmental protection with minimal resource consumption and no pollution emissions.

(2) The invention comprehensively considers all possible cases of catalyst systems and provides full coverage of potential configurations, which is different from blind trial and error experiments and helps to avoid the omission of high-performance catalysts.

(3) The invention adopts progressive screening, which is different from pure experimental inefficient blind trial and error, overcomes the disadvantages of high resource consumption and long research period, and is conducive to narrowing the screening scope and quickly locating potential high-performance catalysts.

(4) The invention conducts computational research based on the firstness principle, which is different from the disadvantages such as high experimental chance and low repeatability, and is characterized by high accuracy and high repeatability.

(5) The invention conducts catalyst research from the atomic scale, revealing the catalytic pathway and mechanism of catalysts from the microscopic perspective, filling the shortcomings of experiments for catalysts with unknown mechanism, which is conducive to guiding experimental synthesis and further promotion and application.

BRIEF DESCRIPTION OF THE DRAWINGS

In order to more clearly illustrate the technical solutions in the embodiments or prior art of the present invention, the following is a brief description of the accompanying drawings to be used in the embodiments, and it is obvious that the accompanying drawings in the following description are only some embodiments of the present invention, and other accompanying drawings can be obtained from these drawings without creative work for those of ordinary skill in the art.

FIG. 1 is a flow chart of the screening of a catalyst for an acid-base all-environment efficient oxygen reduction reaction

DETAILED DESCRIPTION OF THE PREFERRED EMBODIMENTS

To enable a person skilled in the art to better understand the technical solutions of the present invention, the invention is described in further detail below in conjunction with the embodiments.

Example 1

Using $ZnCoN_6$-doped graphene catalyst ($ZnCoN_6$@Gra) as an example.

(1) Construction of $ZnCoN_6$@Gra catalyst pre-screening model by VESTA and optimization of the structure based on the first-nature principle.

(2) Calculating the formation energy ΔE_f=-3.34eV and binding energy ΔE_{b_1}=1.62eV (E_{coh_1}=1.35eV), ΔE_{b_2}=4.71eV (E_{coh_2}=4.39eV); the structure of $ZnCoN_6$@Gra was found to be stable based on ΔE_f <0eV and $\Delta E_b > E_{coh}$.

(3) Constructing the adsorption model of catalyst on O_2 in different adsorption modes and optimizing the structure (the lowest energy adsorption model was selected), calculating the adsorption energy of catalyst on O_2 ΔE_{*O2} = -2.12eV, which indicates the effective adsorption and activation of $ZnCoN_6$@Gra on O_2 according to $\Delta E_{*O2} < -0.5$eV.

(4) Constructing a model for the adsorption of H_2O by the catalyst and optimizing the structure, calculating the adsorption energy of the catalyst on H_2O ΔE_{*H_2O} = -0.54eV, which indicates the weak adsorption of H_2O by $ZnCoN_6$@Gra according to $\Delta E_{*O_2} < \Delta E_{*H_2O}$, which effectively avoids solvent passivation of the catalyst and ensures the recyclability of the catalyst.

(5) The catalyst model was divided into two environments, acidic (pH=0) and basic (pH=14).

a. Acidic environment: consider the possibility of O_2 as ligand modification ($ZnCoN_6O_2$@Gra) based on ΔE_{*O_2}<-1.5eV and proceed to step (3) to continue the screening.

(i) Construct the adsorption model of catalyst for O_2 under different adsorption modes of $ZnCoN_6O_2$@Gra and optimize the structure (choose the lowest energy adsorption model), calculate the adsorption energy of $ZnCoN_6O_2$@Gra for O_2 ΔE_{*O_2}=-0.94eV, according to ΔE_{*O_2}<-0.5eV, $ZnCoN_6O_2$@Gra ensures the effective adsorption and activation of O_2.

(ii) Construct the adsorption model of $ZnCoN_6O_2$@Gra on H_2O and optimize the structure, calculate the adsorption energy of catalyst on H_2O ΔE_{*H_2O}=-0.34eV, according to ΔE_{*O_2}< ΔE_{*H_2O}, which indicates that $ZnCoN_6O_2$@Gra weakly adsorbs on H_2O, which effectively avoids the catalyst from solvent passivation and ensures the recyclability of the catalyst.

(iii) According to ΔE_{*O_2}>-1.5eV, $ZnCoN_6O_2$@Gra has proper adsorption for oxygen.

④ Considering the effect of zero-point vibrational energy and entropy on Gibbs free energy, the OH adsorption model was further calculated and the OH adsorption free energy ΔG_{*OH}=1.12eV was calculated, and according to ΔG_{*OH}>0.4eV it is known that $ZnCoN_6O_2$@Gra is a catalyst with relatively high catalytic activity.

⑤ according to ΔG_{*OH}<1.6eV screening it can be known that $ZnCoN_6O_2$@Gra has a stronger activation of oxygen and higher catalytic activity.

⑥ Calculate the Gibbs free energy of $OOH \rightarrow H_2O_2$ $\Delta G_{*OOH \rightarrow H_2O_2}$=-0.60eV and the reaction energy of the second electron step of the main reaction ΔG_2=-1.76eV, based on $\Delta G_{*OOH \rightarrow H_2O_2} > \Delta G_2$ it is known that $ZnCoN_6O_2$@Gra has low side reaction incidence.

b. Alkaline environment: too strong OH adsorption may passivate the catalyst and make the catalysis difficult to cycle. Construct the model of OH adsorption by catalyst and optimize the structure, calculate the OH adsorption energy ΔE_{*OH}=-3.84eV, according to ΔE_{*OH}<-3.5eV indicates that OH is difficult to desorption, re-enter OH as ligand ($ZnCoN_6OH$@Gra) to continue the screening in step (3).

(i) Construct the adsorption model of catalyst for O_2 under different adsorption modes of $ZnCoN_6OH$@Gra and optimize the structure (choose the lowest energy adsorption model), calculate the adsorption energy of $ZnCoN_6OH$@Gra for O_2 ΔE_{*O_2}=-1.36eV, according to ΔE_{*O_2}<-0.5eV, $ZnCoN_6OH$@Gra ensures the effective adsorption and activation of O_2.

(ii) Constructing the adsorption model of $ZnCoN_6OH$@Gra on H_2O and optimizing the structure, calculating the adsorption energy of catalyst on H_2O ΔE_{*H_2O}=-0.02eV, according to $\Delta E_{*O_2} < \Delta E_{*H_2O}$, indicating that $ZnCoN_6OH$@Gra weakly adsorbs on H_2O, which effectively avoids the catalyst from solvent passivation and ensures the recyclability of the catalyst.

(iii) According to ΔE_{*O_2}>-1.5eV, $ZnCoN_6OH$@Gra has proper adsorption for oxygen.

④ Considering the effect of zero-point vibrational energy and entropy on the Gibbs free energy, the OH adsorption model was further calculated and the OH adsorption free energy ΔG_{*OH} = 0.50 eV was calculated. According to ΔG_{*OH}>0.4 eV it is known that $ZnCoN_6OH$@Gra is a catalyst with relatively high catalytic activity.

⑤ Screening based on ΔG_{*OH}<1.6eV shows that $ZnCoN_6OH$@Gra has a stronger activation of oxygen and higher catalytic activity.

(6) Calculate the Gibbs free energy of $OOH \rightarrow H_2O_2$ $\Delta G_{*OOH \rightarrow H_2O_2}$=-0.18eV and the reaction energy of the second electron step of the main reaction ΔG_2=-1.67eV, based on $\Delta G_{*OOH \rightarrow H_2O_2} > \Delta G_2$ it is known that $ZnCoN_6OH$@Gra has low side reaction incidence.

(6) Calculation of the overpotential η magnitude, η_{acid} = 0.54 V and η_{base} = 0.73 V. According to η_{acid} < 0.8 V and η_{base} < 0.8 V $ZnCoN_6$@Gra is found to be an acid-base all-environment efficient oxygen reduction reaction electrocatalyst.

Contrast ratio 1

1. Precursor strategy for the synthesis of transition metal-doped carbon-based diatomic catalysts

2-Methylimidazole 2-MeIm and zinc nitrate $Zn(NO_3)_2$ were mixed and dissolved in an appropriate amount of methanol CH_3OH solvent by 1:2 mass to prepare ZIF8 solution. Then the transition metal-acetylacetonate compounds $Tm_1(acac)_X$ and $Tm_2(acac)_X$ were added with zinc nitrate by the same mass and stirred for 0.5 h. Then it was transferred to a polytetrafluoroethylene hydrothermal synthesis reactor heated to 120 °C and held for 4 h. The precipitate was obtained by centrifugation at high speed and washed by methanolic CH_3OH, and then dried under vacuum at a constant temperature of 60°C for 12 h to obtain the precursor Tm_1Tm_2@ZIF8 encapsulating $Tm(acac)_X$.

The prepared precursor Tm_1Tm_2@ZIF8 was placed in a tube furnace and heated to 918°C (slightly above the Zn boiling point of 907°C, evaporating Zn while leaving the high boiling point of the transition metal Tm) at a rate of 5°C/min under flowing N_2 and held for 2 hours, and annealed to room temperature with the furnace. Then the powder was acid-washed with 0.5 mol H_2SO_4 for 2 h at room temperature to remove the potential large-size metal material, and finally washed by centrifugation with ultrapure

water and dried under vacuum at 60 ℃ for 12 h to obtain the transition metal-doped porous carbon-based diatomic catalyst.

2. Modern analytical techniques to characterize the microscopic physical phase information of the synthesized catalysts

The BET specific surface area and pore size distribution were determined by nitrogen adsorption instrument. The structure and physical phase of the synthesized catalyst samples were determined by X-ray diffractometer. The microstructure and morphology were observed by transmission electron microscope TEM and scanning electron microscope SEM; the content and distribution of different elements in the synthesized catalysts were detected by X-ray energy spectrum analyzer EDS; and the elemental content of transition metals was accurately determined by inductively coupled plasma mass spectrometer ICP-MS. The overall physical phase information of the catalyst at the microscopic level was obtained by relevant test analysis.

Further information on the active center configuration of the synthesized catalysts can be obtained by high angle annular dark field scanning electron microscopy HAADF-STEM and selected area electron diffraction SAED; X-ray photoelectron spectroscopy (XPS) system was used to test the active center configuration elements and their chemical valence states in the catalyst samples; X-ray absorption near edge spectroscopy (XANES) and extended X-ray absorption fine structure (EXAFS) were used to determine the catalyst content and distribution. XANES and extended X-ray absorption fine structure EXAFS were used to characterize the coordination relationships of the active center configuration. The above-mentioned tests provide comprehensive information on the Tm active site and N-C coordination environment.

3. In situ testing of ORR catalytic performance and mechanism by electrochemistry combined with spectroscopy

A 5 mg sample of catalyst was dispersed in a mixture of 480 μL ethanol, 480 μL H_2O and 40 μL 5% PFOS ethanol solution degraded by acoustic degradation for 0.5 hr. The catalyst was then dropped on a polished glassy carbon rotating disc electrode RDE or rotating disc ring electrode RRDE with diameter d=5 mm and dried at room temperature. The catalyst loading was ~0.5 mg/cm^2.

Tests were performed at room temperature using a three-electrode system with acidic and alkaline environments: the electrolyte was a saturated N_2/O_2 aqueous solution of 0.1 M $HClO_4$ and 0.1 M KOH, respectively, the reference electrode was a saturated glycol electrode SCE, and the counter electrode was a carbon electrode. All measured

potentials were calculated according to Equation (1) and converted to the reversible hydrogen electrode potential RHE.

ERHE = ESCE + 0.059 × pH + 0.2412 V (1).

Firstly, cyclic voltammetry CV scan was carried out to calculate the bilayer capacitance C_{dl} and electrochemical specific surface area ECSA; subsequently, linear scanning voltammetry LSV scan was carried out to obtain the ORR onset potential E_{onset}, half-wave potential $E_{1/2}$ and limiting diffusion current density DLCD, and then the electrocatalytic ORR overpotential η was obtained, and the Tafel slope was obtained by fitting the LSV curve, determining the The reaction limit step RDS was determined by fitting the LSV curve to obtain the Tafel slope, and the charge transfer resistance Rct. The Nyquist plot was obtained based on the electrochemical impedance spectroscopy EIS test, and finally the conversion frequency TOF of the catalyst was investigated by testing the CV curve in neutral phosphate buffered saline PBS.

The electron transfer number n during ORR was calculated from the slope of the Koutecky-Levich (K-L) curve: $j^{-1} = j_k^{-1} + (B\omega 1/2)^{-1}$, $B = 0.62nFC0D0^{2/3}V^{-1/6}$ (2).

Equation (2) in jk and j represent the kinetic control current density at constant potential and the total reaction current density measured, respectively, ω is the rotation rate of the disc electrode, F is the Faraday constant 96485 C/mol, C_0 is the volume concentration of O_2 1.2×10^{-6} mol/cm^3, D_0 is the diffusion coefficient of O_2 in 0.1 M $HClO_4$ or 0.1 M KOH solution 1.9×10^{-5}cm^2/s, and V represents the viscosity of the electrolyte 0.01 cm^2/s. The yield of the side reaction H_2O_2 was calculated based on the electron transfer number n by the relationship between the electron transfer number n and the yield of hydrogen peroxide H_2O_2 shown in Equation 3.

$n=4i_d/(i_d+i_r/N)$, $H_2O_2\%=200id/(i_d\times N+i_r)$ (3).

i_d is the disc current density, i_r is the ring current density, and Pt ring current collection efficiency N=0.37.

Contrast 1 has the following drawbacks.

(1) This existing technology of experimental synthesis, then characterization of the catalyst, and finally electrochemical testing of the performance, due to its unknown nature leads to the possible synthesis of insufficient catalyst performance, resulting in a waste of time, energy, material resources and other resources in various aspects. ②Multiple steps in the test procedure and many variables in the process conditions lead to low reproducibility of the test results. ③Long test cycle, covering catalyst preparation, catalyst characterization, and catalytic performance testing, in addition to subsequent process optimization and performance improvement also face the

disadvantage of long cycle time. ④Multiple test consumables and large "three waste" emissions, including catalyst preparation and catalytic performance testing, and the subsequent optimization of process and performance improvement also face the challenges of many test consumables and large "three waste" emissions. ⑤ The cost of experimental research is high, including catalyst preparation, catalyst characterization and catalytic performance testing, especially catalyst characterization is time-consuming and expensive.

This invention is based on first principles of theoretical calculations, which has the advantages of low resource consumption, low time cost, no pollution emission, high repeatability, and provides accurate guidance for experimental synthesis, thus providing a guarantee for the promotion of hydrogen-oxygen fuel cells. It also effectively enhances the high value-added utilization of mineral resources and the scientific and technological competitiveness of the catalytic industry, helps realize the promotion and application of new energy vehicles, and comprehensively promotes the optimization of energy industry structure and ensures energy security.

The above-described embodiments are only a description of the preferred way of the present invention, not a limitation of the scope of the present invention. Without departing from the spirit of the design of the present invention, all kinds of deformations and improvements made to the technical solutions of the present invention by the ordinary skilled person in the art shall fall within the scope of protection determined by the claims of the present invention.

CLAIMS

1. A method for constructing an acid-base all-environment efficient oxygen reduction reaction electrocatalyst, characterized in that said method is a screening method for N-ligand bimetallic atom co-doped graphene catalysts, comprising the steps：

(1) constructing a pre-screening model for all ORR catalysts;

(2) calculation of formation energy ΔE_f and the binding energy ΔE_b for the pre-screening models; screening the catalyst models based on ΔE_f<0eV and $\Delta E_b > E_{coh}$;

(3) constructing a model for the adsorption of O_2 by the catalyst and calculating the adsorption energy ΔE_{*O2} of the catalyst for O_2; screening the catalyst model based on ΔE_{*O2} < -0.5eV;

(4) constructing a model for the adsorption of H_2O by the catalyst and calculating the adsorption energy of ΔE_{*H2O} by the catalyst; screening the catalyst model according to $\Delta E_{*O2} < \Delta E_{*H2O}$;

(5) classify the catalyst model into two environments, acidic and basic:

a. acidic environment: screen the catalyst based on ΔE_{*O2}>-1.5eV, if ΔE_{*O2}<-1.5eV, proceed to step (3) to continue screening;

b. alkaline environment: construct a model of OH adsorption by the catalyst, calculate the OH adsorption energy ΔE_{*OH}, screen the catalyst based on ΔE_{*OH}>-3.5eV, if ΔE_{*OH}<-3.5eV, proceed to step (3) to continue screening;

(6) calculate the OH adsorption free energy ΔG_{*OH}, plot the overpotential η against the volcano curve of ΔG_{*OH} and screen the catalyst according to ΔG_{*OH}>0.4eV; if ΔG_{*OH}<0.4eV, proceed to step (3) for further screening;

(7) screen the catalyst based on ΔG_{*OH} < 1.6 eV and discard this part of the catalyst if ΔG_{*OH} > 1.6 eV;

(8) calculate the Gibbs free energy $\Delta G_{*OOH \rightarrow H2O2}$ for $OOH \rightarrow H_2O_2$ and the reaction energy ΔG_2 for the second electron step of the main reaction, and screen the catalyst based on $\Delta G_{*OOH \rightarrow H2O2} > \Delta G_2$;

(9) calculate the magnitude of the overpotential η and screen acid-base all-environment efficient oxygen reduction reaction electrocatalysts based on η_{acid} < 0.8 V and η_{base} < 0.8 V.

2. The method for constructing an acid-base all-environment efficient oxygen reduction reaction electrocatalyst according to claim 1, characterized in that step (2) the formation

energy ΔEf is calculated as shown in Eq. 01; the binding energy ΔE_b is calculated as shown in eq. 02 to eq. 03.

$$\Delta E_f=E_{Tm_1Tm_2\text{-}N_x\text{-}C_{6\text{-}x}\text{-}gra}+(4+x)\mu_C-(E_{gra}+x\mu_N+\mu_{Tm_1}+\mu_{Tm_2}) \quad \text{eq.01 ;}$$

$$\Delta E_{b1}=E_{Tm_2\text{-}N_x\text{-}C_{6\text{-}x}\text{-}gra}+\mu_{Tm_1}-E_{Tm_1Tm_2\text{-}N_x\text{-}C_{6\text{-}x}\text{-}gra}$$

eq.02;

$$\Delta E_{b2}=E_{Tm_1\text{-}N_x\text{-}C_{6\text{-}x}\text{-}gra}+\mu_{Tm_2}-E_{Tm_1Tm_2\text{-}N_x\text{-}C_{6\text{-}x}\text{-}gra}$$

eq.03;

among them, $E_{Tm1Tm2\text{-}Nx\text{-}C6\text{-}x\text{-}gra}$ and E_{gra} refer to the system energy of the N-C coordination environment with double T_m atoms in concert to construct doped graphene-based diatomic catalysts and defect-free graphene Gra, respectively; μ_C and μ_N refer to the system energy of a single C atom and 1/2 N_2 molecule in graphene Gra, respectively; μ_{Tm1} and μ_{Tm2} refer to the energy of single-atom metal Tm_1 and Tm_2 respectively; $E_{Tm2\text{-}Nx\text{-}C6\text{-}x\text{-}gra}$ and $E_{Tm1\text{-}Nx\text{-}C6\text{-}x\text{-}gra}$ refer to the system energy of N-C coordination double Tm atom co-doped graphene catalysts with Tm_1 and Tm_2 vacancy defects, respectively.

3. The method for constructing an acid-base all-environment efficient oxygen reduction reaction electrocatalyst according to claim 1, characterized in that step (3) the adsorption energy ΔE_{*O2} of the catalyst for O2 is calculated as shown in eq. 04.

$$\Delta E_{*O_2}= E_{*O_2\text{-}Tm_1Tm_2\text{-}N_x\text{-}C_{6\text{-}x}\text{-}gra} - E_{Tm_1Tm_2\text{-}N_x\text{-}C_{6\text{-}x}\text{-}gra} - E_{O_2} \quad \text{eq.04 ;}$$

$E_{*O2\text{-}Tm1Tm2\text{-}Nx\text{-}C6\text{-}x\text{-}gra}$ is the total system energy of O_2 adsorption by the catalyst and E_{O2} is the energy of a single O_2 molecule.

4. The method for constructing an acid-base all-environment efficient oxygen reduction reaction electrocatalyst according to claim 1, characterized in that step (4) the adsorption energy ΔE_{*H2O} of the catalyst for H_2O is calculated as shown in eq. 05.

$$\Delta E_{*H_2O}= E_{*H_2O\text{-}Tm_1Tm_2\text{-}N_x\text{-}C_{6\text{-}x}\text{-}gra} - E_{Tm_1Tm_2\text{-}N_x\text{-}C_{6\text{-}x}\text{-}gra} - E_{H_2O} \quad \text{eq.05;}$$

$E_{*H2O\text{-}Tm1Tm2\text{-}Nx\text{-}C6\text{-}x\text{-}gra}$ is the total system energy of H_2O adsorption by the catalyst and E_{H2O} is the energy of a single H_2O molecule.

5. The method for constructing an acid-base all-environment efficient oxygen reduction reaction electrocatalyst according to claim 1, characterized in that the OH adsorption energy ΔE_{*OH} of step (5) is calculated as shown in eq. 06.

$$\Delta E_{*OH} = E_{*OH\text{-}Tm_1Tm_2\text{-}N_x\text{-}C_{6-x}\text{-}gra} - E_{Tm_1Tm_2\text{-}N_x\text{-}C_{6-x}\text{-}gra} - E_{OH} \quad \text{eq.06;}$$

$E_{*OH\text{-}Tm1Tm2\text{-}Nx\text{-}C6\text{-}x\text{-}gra}$ is the total system energy of OH adsorption by the catalyst and EOH is the energy of a single OH.

6. The method for constructing an acid-base all-environment efficient oxygen reduction reaction electrocatalyst according to claim 1, characterized in that the OH adsorption free energy ΔG*OH of step (6) is calculated as shown in eq. 07.

$$\Delta G_{*OH} = G_{*OH\text{-}Tm_1Tm_2\text{-}N_x\text{-}C_{6-x}\text{-}gra} - G_{Tm_1Tm_2\text{-}N_x\text{-}C_{6-x}\text{-}gra} - (G_{H_2O} - 1/2G_{H_2}) \quad \text{eq.07}$$

$G_{*OH\text{-}Tm1Tm2\text{-}Nx\text{-}C6\text{-}x\text{-}gra}$ and $G_{Tm1Tm2\text{-}Nx\text{-}C6\text{-}x\text{-}gra}$ are the Gibbs free energies of the system with OH adsorbed by the catalyst and the system with the catalyst alone, respectively, and G_{H2O} and G_{H2} are the Gibbs free energies of individual H_2O and H_2 molecules, respectively.

7. The method for constructing an acid-base all-environment efficient oxygen reduction reaction electrocatalyst according to claim 1, characterized in that the Gibbs free energy $\Delta G_{*OOH\rightarrow H2O2}$ for step (8) $OOH \rightarrow H_2O_2$ and the reaction energy ΔG2 for the second electron step of the main reaction are calculated as shown in eq. 08 and eq. 09.

$$\Delta G_{*OOH\rightarrow H_2O_2} = G_{H_2O_2} + G_{Tm_1Tm_2\text{-}N_x\text{-}C_{6-x}\text{-}gra} - (G_{*OOH\text{-}Tm_1Tm_2\text{-}N_x\text{-}C_{6-x}\text{-}gra} + (0.5G_{H_2} - 0.0592\times pH))$$

eq.08;

$$\Delta G_2 = G_{*O\text{-}Tm_1Tm_2\text{-}N_x\text{-}C_{6-x}\text{-}gra} + G_{H_2O} - (0.5G_{H_2} - 0.0592\times pH) - G_{*OOH\text{-}Tm_1Tm_2\text{-}N_x\text{-}C_{6-x}\text{-}gra} \quad \text{eq.09}$$

$G_{*OOH\text{-}Tm1Tm2\text{-}Nx\text{-}C6\text{-}x\text{-}gra}$ and $G_{*O\text{-}Tm1Tm2\text{-}Nx\text{-}C6\text{-}x\text{-}gra}$ refer to the Gibbs free energy of the system in which the catalyst adsorbs OOH and O, respectively, and G_{H2O2} refers to the Gibbs free energy of a single H_2O_2 molecule.

8. The method for constructing an acid-base all-environment efficient oxygen reduction reaction electrocatalyst according to claim 1, characterized in that step (9) η acid and η base are calculated as shown in eq. 10~ eq. 12 as follows.

$$\Delta G=\Delta E_{DFT}+\Delta ZPE-T\Delta S+\Delta G_U+\Delta G_{pH} \quad \text{eq.10;}$$

$$\eta_{酸}= 1.23\ V + [\Delta G_1, \Delta G_2, \Delta G_3, \Delta G_4]_{max}/e \quad \text{eq.11;}$$

$$\eta_{碱}=0.402\ V + [\Delta G_1, \Delta G_2, \Delta G_3, \Delta G_4]_{max}/e \quad \text{eq.12;}$$

ΔE_{DFT} is the reaction energy based on DFT calculations, ΔZPE and ΔS are the change in zero-point vibrational energy and entropy before and after the reaction, respectively, T is the temperature, and ΔG_U and ΔG_{pH} are the effect of potential and pH on the reaction free energy ΔG, respectively.

9. The method for constructing an acid-base all-environment efficient oxygen reduction reaction electrocatalyst according to claim 8, characterized in that ΔG_U and ΔG_{pH} are calculated as shown in eq. 13 and eq. 14.

$$\Delta G_U=-neU \quad \text{eq.13;}$$

$$\Delta G_{pH}=k_BT\times\ln10\times pH \quad \text{eq.14 ;}$$

n is the number of electron transfers; U is the applied potential and kB is the Boltzmann constant.

REVENDICATIONS

1. Procédé de construction de l'électrocatalyseur pour la réaction d'oxydo-réduction efficace en milieu acide et basique, caractérisé en ce que, il est un procédé de criblage du catalyseur à base de graphène co-dopé par des atomes bimétalliques N-ligandé, comprenant les étapes suivantes :

(1) construire un modèle de pré-criblage pour tous les catalyseurs ORR ;

(2) calculer l'énergie de formation ΔE_f et l'énergie de liaison ΔE_b pour ledit modèle de pré-criblage ; ensuite, cribler le modèle de catalyseur selon $\Delta E_f<0eV$ et $\Delta E_b>E_{coh}$;

(3) construire un modèle d'adsorption de O_2 par le catalyseur, et calculer l'énergie d'adsorption de O_2 ΔE_{*O_2} par le catalyseur ; ensuite, cribler le modèle de catalyseur selon $\Delta E_{*O_2}<-0,5eV$;

(4) construire un modèle d'adsorption de H_2O par le catalyseur, et calculer l'énergie d'adsorption de H_2O ΔE_{*H_2O} par le catalyseur ; ensuite, cribler le modèle de catalyseur selon $\Delta E_{*O_2}<\Delta E_{*H_2O}$;

(5) classer le modèle de catalyseur suivant le milieu acide et le milieu basique :

a. pour le milieu acide : cribler le catalyseur selon $\Delta E_{*O_2}>-1,5eV$; dans le cas où $\Delta E_{*O_2}<-1,5eV$, passer à l'étape (3) pour continuer le criblage ;

b. pour le milieu basique : construire un modèle d'adsorption de OH par le catalyseur, et calculer l'énergie d'adsorption de OH ΔE_{*OH} ; ensuite, cribler le catalyseur selon $\Delta E_{*OH}>-3,5eV$; dans le cas où $\Delta E_{*OH}<-3,5eV$, passer à l'étape (3) pour continuer le criblage ;

(6) calculer l'énergie libre d'adsorption de OH ΔG_{*OH}, et dessiner la courbe volcanique du surpotentiel η et du paramètre ΔG_{*OH} ; ensuite, cribler le catalyseur selon $\Delta G_{*OH}>0,4eV$; dans le cas où $\Delta G_{*OH}<0,4eV$, passer à l'étape (3) pour continuer le criblage ;

(7) cribler le catalyseur selon $\Delta G_{*OH}<1,6eV$; dans le cas où $\Delta G_{*OH}>1,6eV$, rejeter le catalyseur correspondant ;

(8) calculer l'énergie libre de Gibbs de $OOH \rightarrow H_2O_2$ $\Delta G_{*OOH \rightarrow H_2O_2}$ ainsi que l'énergie de réaction ΔG_2 pour la deuxième étape électronique de la réaction principale, et cribler le catalyseur selon $\Delta G_{*OOH \rightarrow H_2O_2}>\Delta G_2$;

(9) calculer le surpotentiel η, et selon $\eta_{acide}<0,8V$ et $\eta_{base}<0,8V$, cribler l'électrocatalyseur pour la réaction d'oxydo-réduction efficace en milieu acide et basique.

2. Procédé de construction de l'électrocatalyseur pour la réaction d'oxydo-réduction efficace en milieu acide et basique selon la revendication 1, caractérisé en ce que, à l'étape (2), ladite énergie de formation ΔE_f est calculée selon l'eq.01 ci-dessous ; et ladite énergie de liaison ΔE_b est calculée selon l'eq.02 et l'eq.03 ci-dessous :

$$\Delta E_f = E_{Tm_1Tm_2\text{-}N_x\text{-}C_{6-x}\text{-}gra} + (4+x)\,\mu_C - (E_{gra} + x\mu_N + \mu_{Tm_1} + \mu_{Tm_2}) \quad \text{eq.01;}$$

$$\Delta E_{b1} = E_{Tm_2\text{-}N_x\text{-}C_{6-x}\text{-}gra} + \mu_{Tm_1} - E_{Tm_1Tm_2\text{-}N_x\text{-}C_{6-x}\text{-}gra} \quad \text{eq.02;}$$

$$\Delta E_{b2} = E_{Tm_1\text{-}N_x\text{-}C_{6-x}\text{-}gra} + \mu_{Tm_2} - E_{Tm_1Tm_2\text{-}N_x\text{-}C_{6-x}\text{-}gra} \quad \text{eq.03;}$$

où : $E_{Tm_1Tm_2\text{-}N_x\text{-}C_{6-x}\text{-}gra}$ et E_{gra} désignent respectivement l'énergie du système du catalyseur diatomiques à base de graphène co-dopé par un double atome de Tm N-C ligandé, et celle du système du graphène Gra sans défaut ; μ_C et μ_N désignent respectivement l'énergie du système d'un seul atome de C dans le graphène Gra, et celle du système de la 1/2 molécule N_2 ; μ_{Tm_1} et μ_{Tm_2} désignent respectivement l'énergie du métal monatomique Tm_1 et celle du métal monatomique Tm_2 ; $E_{Tm_2\text{-}N_x\text{-}C_{6-x}\text{-}gra}$ et $E_{Tm_1\text{-}N_x\text{-}C_{6-x}\text{-}gra}$ désignent respectivement l'énergie du système du catalyseur à base de graphène co-dopé par un double atome de Tm N-C ligandé en présence d'un défaut Tm_1, et celle du système dudit catalyseur en présence d'un défaut Tm_2.

3. Procédé de construction de l'électrocatalyseur pour la réaction d'oxydo-réduction efficace en milieu acide et basique selon la revendication 1, caractérisé en ce que, à l'étape (3), ladite énergie d'adsorption de O_2 ΔE_{*O_2} par le catalyseur est calculée selon l'eq.04 ci-dessous :

$$\Delta E_{*O_2} = E_{*O_2\text{-}Tm_1Tm_2\text{-}N_x\text{-}C_{6-x}\text{-}gra} - E_{Tm_1Tm_2\text{-}N_x\text{-}C_{6-x}\text{-}gra} - E_{O_2} \quad \text{eq.04;}$$

où : $E_{*O_2\text{-}Tm_1Tm_2\text{-}N_x\text{-}C_{6-x}\text{-}gra}$ désigne l'énergie totale du système pour l'adsorption de O_2 par le catalyseur ; et E_{O_2} désigne l'énergie d'une seule molécule d'O_2.

4. Procédé de construction de l'électrocatalyseur pour la réaction d'oxydo-réduction efficace en milieu acide et basique selon la revendication 1, caractérisé en ce que, à l'étape (4), ladite énergie d'adsorption de H_2O ΔE_{*H_2O} par le catalyseur est calculée selon l'eq.05 ci-dessous :

$$\Delta E_{*H_2O} = E_{*H_2O\text{-}Tm_1Tm_2\text{-}N_x\text{-}C_{6-x}\text{-}gra} - E_{Tm_1Tm_2\text{-}N_x\text{-}C_{6-x}\text{-}gra} - E_{H_2O} \quad \text{eq.05;}$$

où : $E_{*H_2O\text{-}Tm_1Tm_2\text{-}N_x\text{-}C_{6-x}\text{-}gra}$ désigne l'énergie totale du système pour l'adsorption de H_2O par le catalyseur ; et E_{H_2O} désigne l'énergie d'une seule molécule de H_2O.

5. Procédé de construction de l'électrocatalyseur pour la réaction d'oxydo-réduction efficace en milieu acide et basique selon la revendication 1, caractérisé en ce que, à l'étape (5), ladite énergie d'adsorption de OH ΔE_{*OH} par le catalyseur est calculée selon l'eq.06 ci-dessous :

$$\Delta E_{*OH} = E_{*OH\text{-}Tm_1Tm_2\text{-}N_x\text{-}C_{6\text{-}x}\text{-}gra} - E_{Tm_1Tm_2\text{-}N_x\text{-}C_{6\text{-}x}\text{-}gra} - E_{OH} \quad \text{eq.06;}$$

où : $E_{*OH\text{-}Tm_1Tm_2\text{-}N_x\text{-}C_{6\text{-}x}\text{-}gra}$ désigne l'énergie totale du système pour l'adsorption de OH par le catalyseur ; et E_{OH} désigne l'énergie d'une seule molécule de OH.

6. Procédé de construction de l'électrocatalyseur pour la réaction d'oxydo-réduction efficace en milieu acide et basique selon la revendication 1, caractérisé en ce que, à l'étape (6), ladite énergie d'adsorption de OH ΔG_{*OH} par le catalyseur est calculée selon l'eq.07 ci-dessous :

$$\Delta G_{*OH} = G_{*OH\text{-}Tm_1Tm_2\text{-}N_x\text{-}C_{6\text{-}x}\text{-}gra} - G_{Tm_1Tm_2\text{-}N_x\text{-}C_{6\text{-}x}\text{-}gra} - (G_{H_2O} - 1/2G_{H_2}) \quad \text{eq.07;}$$

où : $G_{*OH\text{-}Tm_1Tm_2\text{-}N_x\text{-}C_{6\text{-}x}\text{-}gra}$ et $G_{Tm_1Tm_2\text{-}N_x\text{-}C_{6\text{-}x}\text{-}gra}$ désignent respectivement l'énergie libre de Gibbs du système pour l'adsorption de OH par le catalyseur, et celle du système de catalyseur unique ; G_{H_2O} et G_{H_2} désignent respectivement l'énergie libre de Gibbs d'une seule molécule de H_2O, et celle d'une seule molécule de H_2.

7. Procédé de construction de l'électrocatalyseur pour la réaction d'oxydo-réduction efficace en milieu acide et basique selon la revendication 1, caractérisé en ce que, à l'étape (8), ladite énergie libre de Gibbs de $OOH \rightarrow H_2O_2$ $\Delta G_{*OOH \rightarrow H_2O_2}$ ainsi que ladite énergie de réaction ΔG_2 pour la deuxième étape électronique de la réaction principale sont calculées selon l'eq.08 et l'eq.09 ci-dessous :

$$\Delta G_{*OOH \rightarrow H_2O_2} = G_{H_2O_2} + G_{Tm_1Tm_2\text{-}N_x\text{-}C_{6\text{-}x}\text{-}gra} - (G_{*OOH\text{-}Tm_1Tm_2\text{-}N_x\text{-}C_{6\text{-}x}\text{-}gra} + (0.5G_{H_2} - 0.0592 \times pH))$$

eq.08;

$$\Delta G_2 = G_{*O\text{-}Tm_1Tm_2\text{-}N_x\text{-}C_{6\text{-}x}\text{-}gra} + G_{H_2O} - (0.5G_{H_2} - 0.0592 \times pH) - G_{*OOH\text{-}Tm_1Tm_2\text{-}N_x\text{-}C_{6\text{-}x}\text{-}gra}$$

eq.09 ;

où : $G_{*OOH\text{-}Tm_1Tm_2\text{-}N_x\text{-}C_{6\text{-}x}\text{-}gra}$ et $G_{*O\text{-}Tm_1Tm_2\text{-}N_x\text{-}C_{6\text{-}x}\text{-}gra}$ désignent respectivement l'énergie libre de Gibbs du système pour l'adsorption de OOH et de O par le catalyseur ; $G_{H_2O_2}$ désigne l'énergie libre de Gibbs d'une seule molécule de H_2O_2.

8. Procédé de construction de l'électrocatalyseur pour la réaction d'oxydo-réduction efficace en milieu acide et basique selon la revendication 1, caractérisé en ce que, à l'étape (9), lesdits η_{acide} et η_{base} sont calculés selon l'eq.10 à l'eq.12 ci-dessous :

$\Delta G=\Delta E_{DFT}+\Delta ZPE-T\Delta S+\Delta G_U+\Delta G_{pH}$ eq.10;

$\eta_{acide}= 1.23\ V + [\Delta G_1, \Delta G_2, \Delta G_3, \Delta G_4]_{max}/e$ eq.11;

$\eta_{base}=0.402\ V + [\Delta G_1, \Delta G_2, \Delta G_3, \Delta G_4]_{max}/e$ eq.12;

où : ΔE_{DFT} désigne l'énergie de réaction obtenue sur la base de calculs DFT ; ΔZPE et ΔS désignent respectivement les variations de l'énergie vibratoire du point zéro et de l'entropie avant et après la réaction ; T désigne la température ; ΔG_U et ΔG_{pH} désignent respectivement les effets du potentiel et du pH sur l'énergie libre de réaction ΔG.

9. Procédé de construction de l'électrocatalyseur pour la réaction d'oxydo-réduction efficace en milieu acide et basique selon la revendication 8, caractérisé en ce que, lesdits ΔG_U et ΔG_{pH} sont calculés selon l'eq.13 et l'eq.14 ci-dessous :

$\Delta G_U=-neU$

eq.13;

$\Delta G_{pH}=k_BT\times ln10\times pH$ eq.14;

où : n désigne le nombre de transferts d'électrons ; U désigne le potentiel externe ; et k_B désigne la constante de Boltzmann.

FIGURES

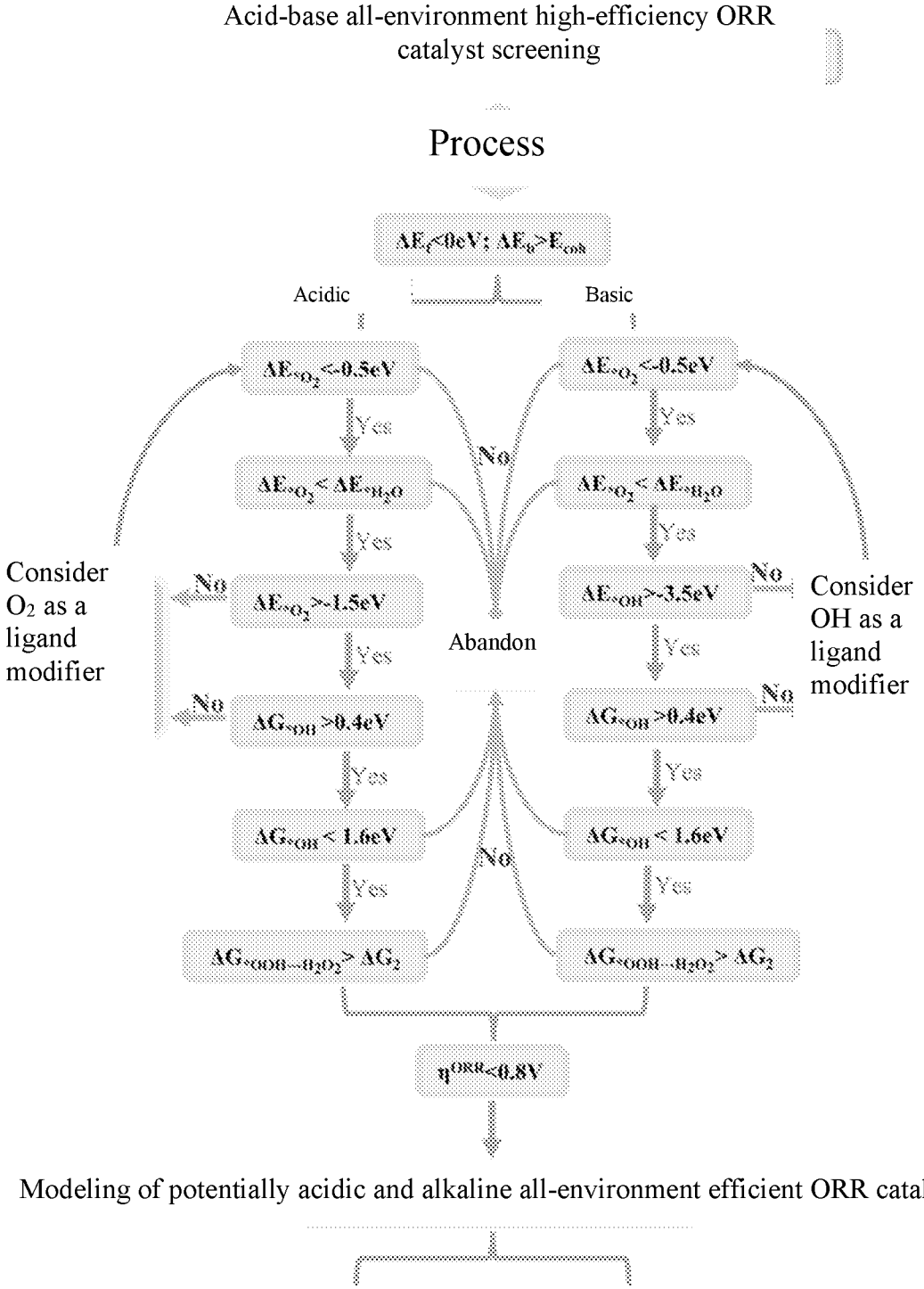

FIG.1